Surface modification of low density polyethylene in a fluorine gas plasma

M. Anand, R. E. Cohen and R. F. Baddour
Department of Chemical Engineering, Massachusetts Institute of Technology, Cambridge, Massachusetts 02139, *USA*
(*Received* 27 *March* 1980; *revised* 6 *June* 1980)

Low density polyethylene was fluorinated in a glow discharge generated from a dilute mixture of fluorine in helium. The effects of pressure, flow rate, power and time of treatment have been examined. The fluorinated polymers were characterized using e.s.c.a. to identify the species present in the surface layer and to estimate the depth of fluorination. For typical plasma treatment of polyethylene films the fluorination depth was about 40 Å; a competition of ablation and ion-assisted etching processes with chemical reaction was observed. The depth of fluorination was increased to values above 60 Å by carrying out the reaction within a metal screen. The presence of the screen also reduced the reaction rate by about a factor of two. Other features of the treated polyethylene were determined by contact angle measurements, surface infra-red spectroscopy, solvent sorption and differential scanning calorimetry. Some early results of treatment of polyethylene powders in a fluidized bed reactor are also presented.

INTRODUCTION

Numerous studies have been reported[1-7] of perfluorination of hydrocarbon polymers by direct reaction with elemental fluorine. These studies, largely directed toward fluorinating the polymers in bulk, employed long reaction times and high concentrations of fluorine. Fredericks and Tedder suggested that progression of fluorination becomes increasingly difficult in the case of polyethylene because a substituent fluorine deactivates the adjacent hydrogen atoms in the free radical reaction[8]. The propagation of the reaction into the bulk of polyethylene is known to be diffusion controlled[9,10], requiring greater concentrations of fluorine as the depth of fluorination increases. Some reactions of polymers with fluorine gas in high concentrations have also been observed to promote cross-linking and degradation[2,4].

Recent research efforts by Clark *et al.*[10,11] and by Shimada and Hoshino[9] have attempted to study fluorination of the surface and subsurface layers of hydrocarbon polymers by substitution reaction with fluorine atoms. They have elucidated some features concerning the mechanism and kinetics of the initial phase of the reaction and have studied parameters affecting diffusivity of the reactant into the subsurface layers. Clark and coworkers[10] have used e.s.c.a. measurements as a means for identification of various fluorinated species in the surface layers; the problem of post reaction with oxygen, which leads to formation of oxygen-containing species on the surface of the treated polyethylene, was also revealed in their studies. Alternate approaches at producing perfluorinated layers by carrying out polymerizations of fluorinated monomers have also revealed the problem of formation of several partially fluorinated species[12,15]. Thus, true perfluorination of the surface has not been achieved.

In the present study, we have attempted to accelerate the rate of reaction of fluorine species with polyethylene by using a cold plasma generated from a dilute mixture of fluorine gas in helium. Rapid fluorination may be expected to occur in this case owing to the generation of active fluorine and diluent gas species in the plasma and due to reactive species which are created on the surface of the solid substrate. The source of fluorine radicals (and ions) in the present study was fluorine gas which dissociates readily into F· in a glow discharge. The formation of fluorine anions takes place by further collisions with electrons and other activated particles. Cation formation in the plasma occurs via activation of the diluent gas helium and due to the presence of some impurities which may be desorbed from the polymer or from the walls of the reaction chamber. Active fluorine and fluorine-containing species can also be generated from other sources, such as CF_4, C_2F_6 and SF_6. A recent patent by Manion and Davies[16] discusses the effect of various plasma parameters such as power and pressure on the surface fluorination of cotton and polyethylene in CF_4 plasma.

EXPERIMENTAL METHODS

The apparatus used for surface fluorination is shown in *Figure 1a*. The plasma is generated by inductively coupling the reactor to a radio frequency generator (LFE Corp.) operating at a frequency of 13.56 MHz. The generator is equipped with an auto-tuner which minimizes the reflected power. Low density polyethylene (LDPE) film (~50 μm thick) supplied by Dow Chemical Company (PE-303) was employed as received for experiments on strip samples. Certain experiments were carried out using film samples enclosed in a cage, a tubular aluminium screen which was placed into the reactor and around the sample carousel. Some experiments were conducted on LDPE powders which were obtained by cryogenic grinding of Dow PE 120 resin. These latter experiments were carried out in a fluidized bed reactor in an attempt to achieve uniform treatment of the powders. The fluidized bed was

0032-3861/81/030361-11$02.00
©1981 IPC Business Press

supported on a fritted glass bottom in a pyrex reactor (*Figure 1b*).

In a typical run, the reaction chamber was evacuated for 12 h, after which dilute fluorine (5% F_2, 95% He) was introduced into the system. When the pressure and flow rate in the chamber had stabilized to the desired values (always within 2 min), the plasma was ignited and maintained for a specified treatment time, after which the system was quickly flushed with helium at 10 mmHg.

Analysis of the surfaces of the polymers was carried out using several complementary techniques. X-ray photoelectron spectroscopy (X.p.s. or e.s.c.a.; Physical Electronics Model 548) was used extensively at low and high resolutions to obtain: (i) an overall chemical analysis in terms of atomic % species by measuring the areas under the 1*s* peaks[17], (ii) an approximate estimate of depth of fluorination by using area ratios of F_{1s} and F_{2s} photoelectron peaks[10], (iii) identification of various fluorinated species by means of chemical shifts in the C_{1s} spectra[10,13,18], (iv) an indication of an 'average' composition by measurement of the Auger parameter[17], (v) charging characteristics as related to chemical structure. It is important to point out here that experimental methods were not employed to eliminate sample charging (e.g. by using a neutralizer filament), and so the CH_2–CH_2 C_{1s} peak from polyethylene was shifted to a location of 285.0 eV on the binding energy scale. All the other C_{1s} spectra were shifted correspondingly.

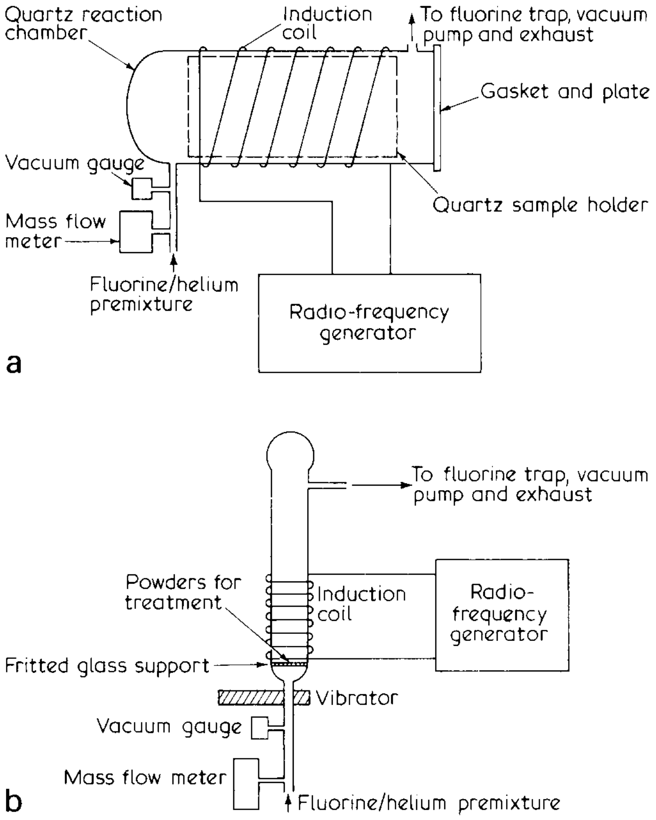

Figure 1 Schematic of experimental set-up; (a) reactor for film treatment, (b) fluidized bed reactor for treatment of powders

In addition to e.s.c.a., Fourier Transform Multiple Internal Reflectance infra-red spectroscopy (Digilab FTS-14) was used for identification of various chemical groups. Spectra were taken under grazing conditions (30°) where it is estimated that information may be obtained to a depth of about 10 000 Å[19,20]. A variable angle *MIR* attachment (Wilks Scientific Model 50) was used for these experiments. Information on the first molecular layer was obtained by measuring the advancing contact angle on the treated polymer using formamide as a contacting liquid.

Additional characterization of the treated polymer films and powders was carried out using scanning electron microscopy (*SEM*), solvent sorption (*SS*) experiments[21,22] and differential scanning calorimetry (d.s.c.). Finally, the moulding of the treated powders was studied as a function of temperature at various pressures of up to ≈350 MPa in an isostatic press.

RESULTS

Pressure, flow rate, applied power, time of treatment, and location of specimen with respect to the plasma zone are parameters which may be expected to influence the surface treatment. The range of reaction conditions employed in our experiments is summarized in *Table 1*.

The effect of these parameters was studied in terms of the extent of fluorination which is reported here as atomic percent fluorine, obtained by area measurements of 1*s* peaks from e.s.c.a. spectra (see Appendix I). The composite effect of pressure and flow rate as a function of time of treatment with and without plasma is shown in *Figure 2*. At high flow rates and pressures, fluorination proceeds very rapidly and reaches the maximum level of fluorination in time scales as small as 30 s; at low flow rates and pressures (10 cc min^{-1}, 1.0 mm), the rate of reaction is slow and there is a small maximum in atomic percent fluorine observed at short reaction times. At 2.0 mm, the extent of fluorination is lower with elemental fluorine compared to plasma treatment. The significance of these observations will be discussed later in the paper.

Table 1 Range of reaction conditions

Specimen type	Pressure (mm Hg)	Flow rate (cm^3 min^{-1})	Applied power* (W)	Time of treatment	Location of specimens	Comments
Film	1–3	10–50	25–100	15 s to 1 h	(1) under *rf* coil (2) within metal cage and under coil	Specimens are placed within the uniform plasma region
Powder	~10	10–40	25–100	15 s to 15 min	Just upstream of coil	The bed of powder was vibrated and fluidized to about two times original bed depth

* Reflected power is essentially zero

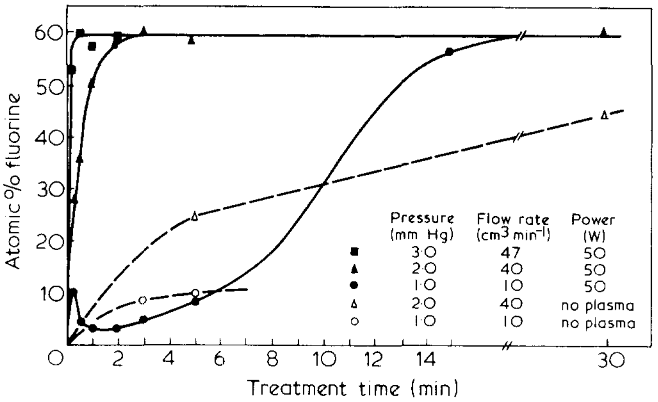

Figure 2 The combined effect of flow rate and pressure on the extent of fluorination as a function of time of treatment as measured by e.s.c.a.

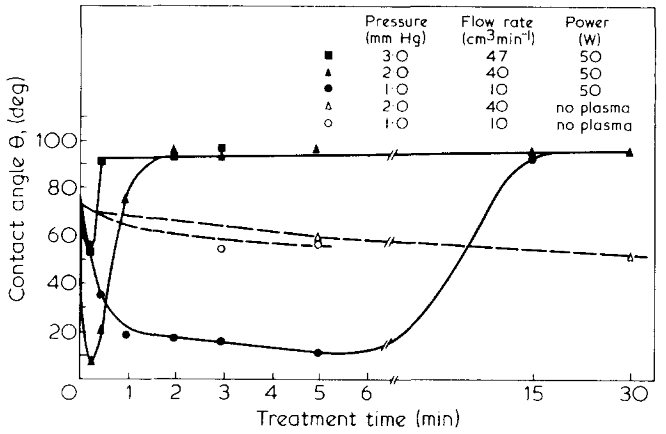

Figure 3 Variation of advancing contact angle (formamide) with time of treatment corresponding to reactions of *Figure 2*

Two other sets of results that complement *Figure 2* are change in contact angle with extent of fluorination and extent of oxidation on the surface as fluorination proceeds. The variations in contact angle and atomic percent oxygen on the surface are shown in *Figures 3* and *4* respectively. The contact angle and amount of oxygen on the surface follow an inverse relationship. This is expected because an increase in oxygen content would increase wettability of the surface and hence reduce the contact angle. A sharp maximum and a corresponding minimum are observed in the oxygen content and in the contact angle plots respectively. Further, in some cases polyethylene films treated in the plasma show higher oxygen contents than those without the plasma, even though fluorine contents are comparable. This effect is observable only for incomplete surface fluorination, and is greatly emphasized for reactions at low pressures and flow rates (*Table 2*).

The effect of power (supplied to the plasma) on the extent of fluorination was studied in the range of 25–100 W power as indicated in *Table 1*. The results are summarized in *Figure 5*. Over this range of power there was little change in the level of fluorination. The rest of the experimental results reported were obtained at a power level of 50 W.

The individual effects of flow rate and pressure on the extent of fluorination and contact angle are depicted in *Figures 6* and *7* respectively. The important region to observe is between 20 and 30 cm^3 min^{-1}. It seems that there is a minimum flow rate of ~40 cm^3 min^{-1} necessary to achieve rapid fluorination. Therefore for small reaction times, it is necessary to utilize large flow rates of fluorine through the system. This phenomenon may be explained according to suggestions of Clark and Dilks[23]: an increased flow rate will result in greater efficiency in the removal of volatile products of reaction, namely, H_2, HF causing a decrease in their partial pressures in the immediate vicinity of the sample. This will tend to increase the rate of reaction.

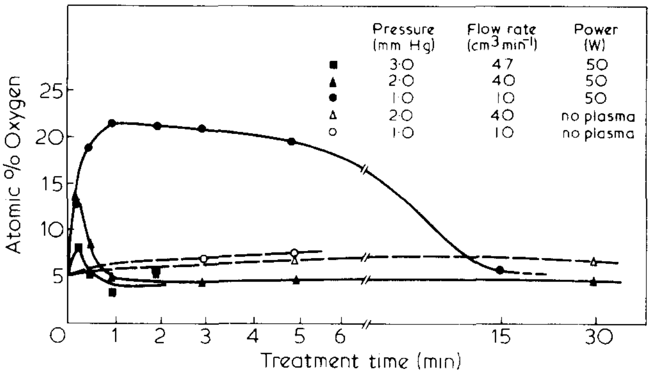

Figure 4 Oxygen content on the surface of fluorinated LDPE for reactions of *Figure 2*

Table 2 Comparison of oxygen contents for treatments at low pressures and flow rates

Reaction conditions	Atomic % F	Atomic % O
5 min, 1 mm, 10 cm^3 min^{-1} no plasma	9.3	7.1
5 min, 1 mm, 10 cm^3 min^{-1} 50 W	8.5	19.6
3 min, 1 mm, 10 cm^3 min^{-1} no plasma	8.8	6.5
3 min, 1 mm, 10 cm^3 min^{-1} 50 W	7.0	19.3

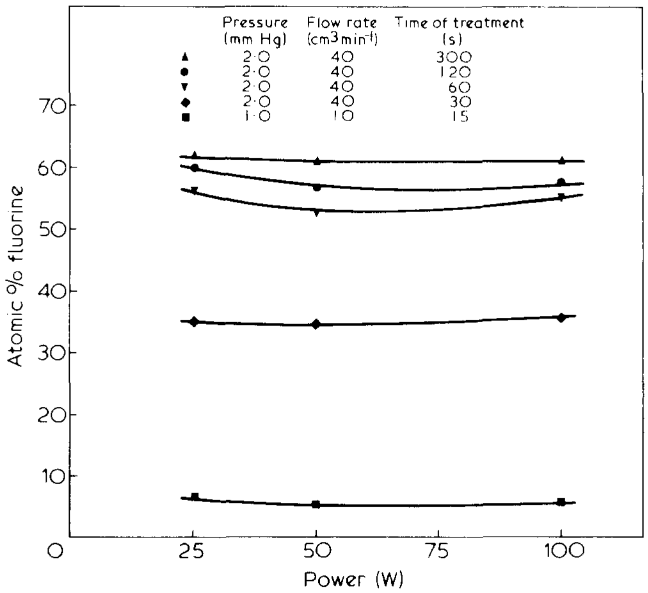

Figure 5 Effect of power on extent of fluorination as measured by e.s.c.a.

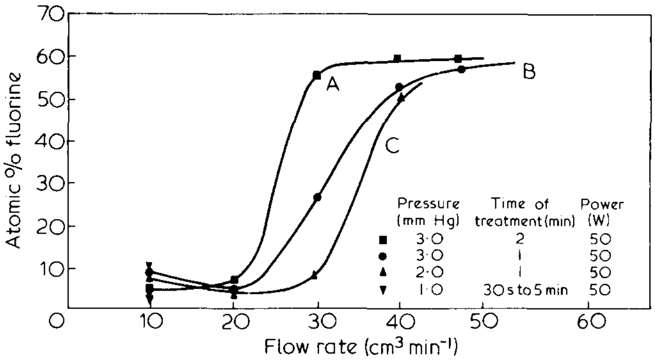

Figure 6 Effect of flow rate on extent of fluorination. Also notice the effect of pressure at constant flow rates

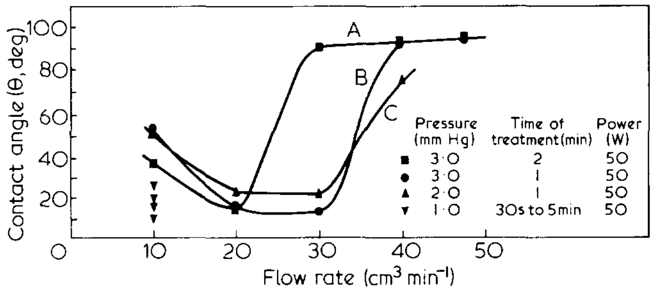

Figure 7 Variation of contact angle (with formamide) for conditions of *Figure 6*

The effect of pressure can also be visualized from curves (B) and (C) of *Figure 6*. In the region in which substantial reaction occurs, increasing the pressure from 2.0 mm to 3.0 mm causes the reaction rate to increase. This is to be expected because increase in pressure is equivalent to an increase in the concentration of the reactive fluorine species which would lead to an increased reaction rate.

The variation of contact angle for the measurements reported in *Figure 6* is shown in *Figure 7*. The reaction profiles in *Figure 7* are consistent with those of *Figure 6*.

DISCUSSION

Characterization of the fluorinated polymer film. Detailed chemical characterization of the plasma treated polyethylene film was carried out by advancing contact angle measurements (first molecular layer), e.s.c.a. ($\sim$50 Å depth), *FTMIR* i.r. ($\sim$10000 Å depth). The information obtained from each of these techniques is discussed individually in the following sections.

Contact angle measurements

By using a set of well characterized contacting liquids in contact angle measurements, the dispersion and polar components of the surface energy can be obtained[24]. In this paper we present contact angle values with one liquid only, formamide, because it has a good balance between polar and dispersion surface tensions. The contact angle, in addition to being sensitive to surface chemical groups is also sensitive to surface morphology[24]. However, in our experiments, the plasma treatment did not appear to change the surface morphology as observed in an *SEM* (*Figure 8*). Thus, changes in contact angle in our experiments are attributed to chemical modifications on the surface. The range of contact angles is shown in *Table 3*.

A reduction in contact angle below the value for untreated LDPE mirrors the observed increase in oxygen on the surface, consistent with wettability ideas. Increased oxygen contents were observed for surface reaction which had not gone to completion (*Figures 3* and *4*, *Table 3*). We interpret this in terms of a post reaction between the polymer and oxygen or oxygen-containing species. A likely source for these species is water molecules from the atmosphere which are chemisorbed onto the acidic sites that may be produced due to partial fluorination. This effect was more dramatically observed in the case of partially fluorinated powders produced by plasma surface

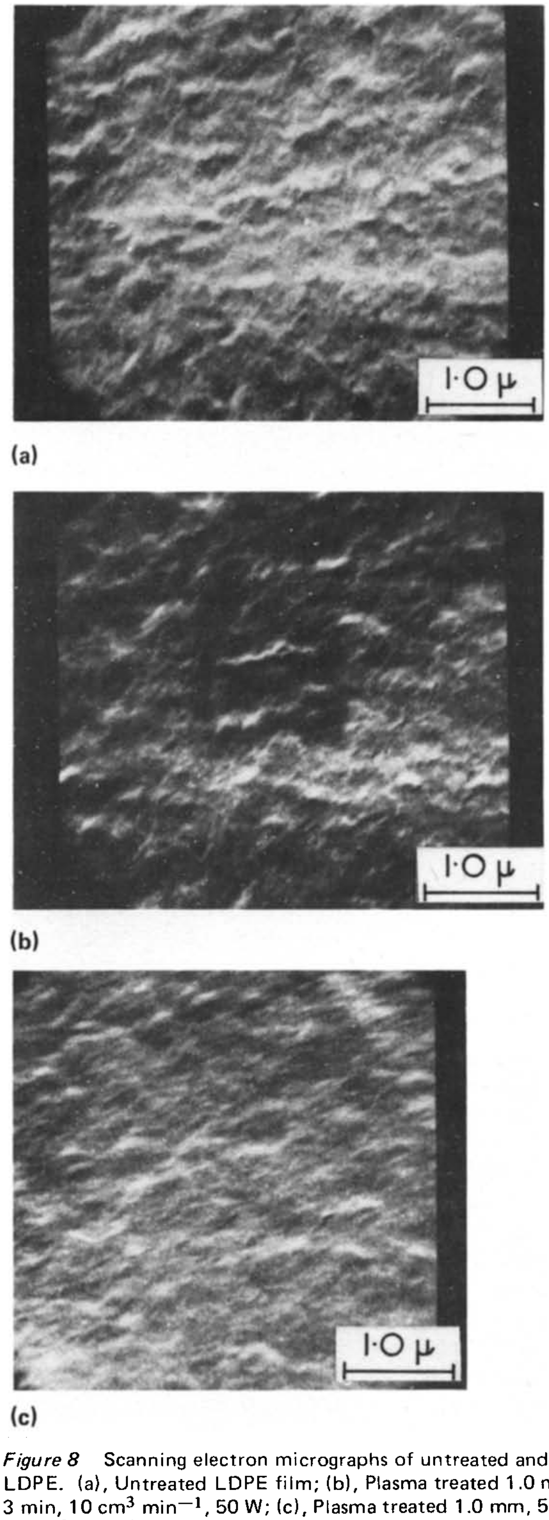

Figure 8 Scanning electron micrographs of untreated and treated LDPE. (a), Untreated LDPE film; (b), Plasma treated 1.0 mm, 3 min, 10 cm^3 min^{-1}, 50 W; (c), Plasma treated 1.0 mm, 5 min, 10 cm^3 min^{-1}, 50 W

Table 3 Range of contact angles typically observed in our experiments

F_2 Plasma treatment	Atomic % O (e.s.c.a.)	Atomic % F (e.s.c.a.)	Contact angle (Formamide)
Untreated LDPE	~5.3	–	71
15 s, 50 W, 2.0 mm, 40 cm^3 min^{-1}	13.7	28.3	~5°
300 s, 50 W, 2.0 min, 40 cm^3 min^{-1}	3.6	61.8	~95°
60 s, 50 W, 3.0 min, 47 cm^3 min^{-1}	3.2	56.6	93.5
120 s, 50 W, 3.0 min, 47 cm^3 min^{-1}	5.8	58.6	~96
PTFE Untreated	1.3	61.0	92
PTFE, 50 W, 2.0 min, 40 cm^3 min^{-1}	–	–	~97

treatment of LDPE powders. This interpretation is supported by the following observations: (i) The powders seemed similar in appearance to moist salt, (ii) A drop in pH was observed when the powders were suspended in distilled water (iii). The charging properties were dramatically altered as observed during e.s.c.a. experiments. (iv) Slight degassing was observed when the X-ray beam was moved to such a specimen during e.s.c.a. experiments. Another explanation for the presence of oxygen on the surface of partially fluorinated PE could be related to a post-reaction of trapped free radicals with oxygen from the atmosphere. The strong argument in favour of this idea is that plasma treated films (for incomplete fluorinations) showed higher oxygen contents than films reacted with elemental fluorine (*Table 2*). This suggests that the reactive species produced play a role in reaction with oxygen. A çombination of the above two processes cannot be ruled out.

In certain cases contact angles were obtained which were greater than the 92° value for PTFE, suggesting the presence of $-CF_3$ groups on the surface. The formation of such groups has been suggested by Nakajima *et al.*[13] and Kay *et al.*[15] in their studies involving polymerization of C_2F_4 in a glow discharge. In our case, $-CF_3$ groups could be formed at chain ends or through scission of C–C bonds leading to an increased number of sites available for formation of $-CF_3$ groups. The importance of CF_3 groups will become apparent in interpretation of some high resolution e.s.c.a. spectra.

E.s.c.a. measurements

Identification of fluorinated species. Previous sections revealed the usefulness of e.s.c.a. in obtaining surface analysis in terms of atomic percent of various species. The applicability of the technique in following the fluorination reaction is shown in *Figure 9* where buildup of fluorine containing species is compared for reactions with and without the plasma. A very important revelation from this set of spectra is that for the case of reaction in the plasma, CF_2 groups are formed very rapidly as concluded from the shifts in binding energy from the initial CH_2–CH_2 position. For the plasma treated samples (spectra on the left in *Figure 9*) there is a chemical shift of ~5–6 eV from the initial position of CH_2–CH_2 at 285.0 eV; peaks in this region are related to signals from $-CF_2$ type groups (Appendix II). However, for the case of reaction with elemental fluorine (spectra on the right in *Figure 9*) several intermediate species including –CHF are formed as observed by the strength of the signal in the intermediate binding energy range of ~287–291 eV. These partially fluorinated species have also been observed in the fluorine gas treatments of HDPE conducted by Clark and coworkers[10]. *Figure 9* clearly suggests that our plasma treatment follows a reaction mechanism which is different from that of reaction of LDPE with elemental fluorine. It appears that in plasma reactions at high flow rates, predominantly CF_2 species are formed; this suggests a situation in which two hydrogens are stripped from each carbon atom followed by reaction with two fluorine radicals.

Another method for verifying the presence of the CF_2 groups is via the Auger parameter which can be useful in giving an estimate of the overall composition of the fluorinated layer. The Auger Parameter, Au_α is defined as:

$$Au_\alpha = BEF_{F_{1s}} - BE_{F_{Au}} + h\nu_{MgK\alpha}$$

where $BE_{F_{1s}}$ = observed binding energy of F_{1s} peak; $BE_{F_{Au}}$ = observed binding energy of fluorine Auger peak; and $h\nu_{MgK\alpha}$ = X-ray (Magnesium source) excitation energy = 1253.6 eV. Some values of Au_α for fluorinated carbon-containing compounds are reported in Wagner *et al.*[17]. The Au_α for $(CF_2)_n$ is 1341 and for CF 1342. Thus depending on the value of Au_α, one may obtain an

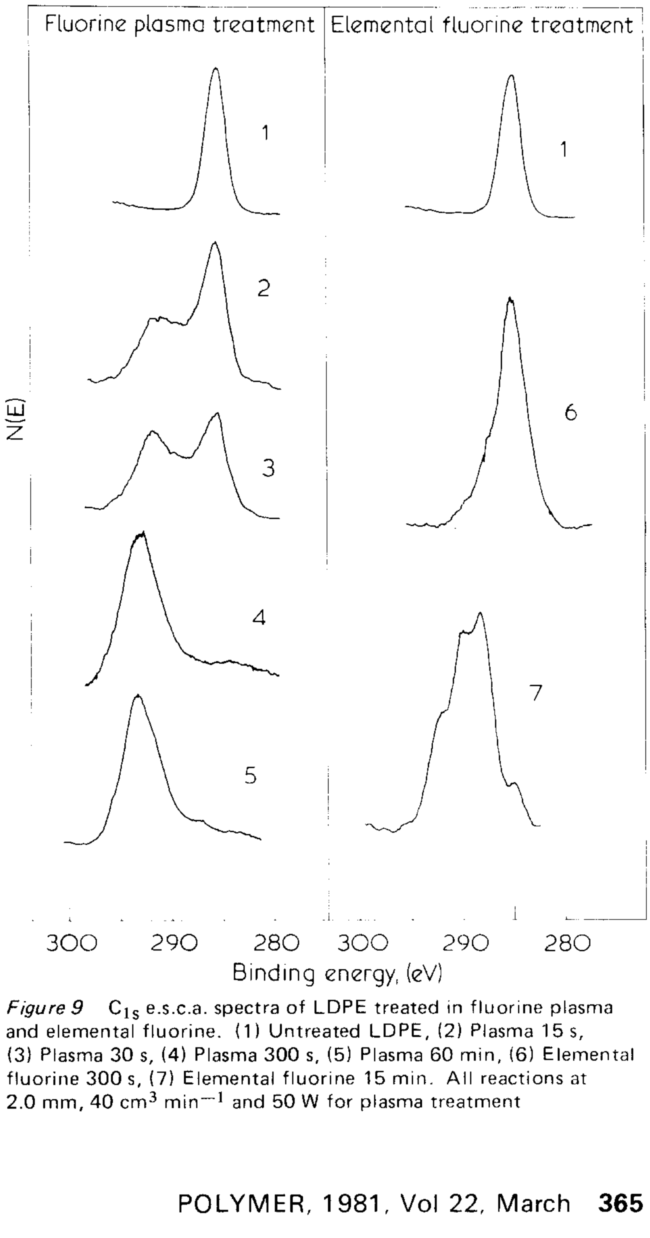

Figure 9 C_{1s} e.s.c.a. spectra of LDPE treated in fluorine plasma and elemental fluorine. (1) Untreated LDPE, (2) Plasma 15 s, (3) Plasma 30 s, (4) Plasma 300 s, (5) Plasma 60 min, (6) Elemental fluorine 300 s, (7) Elemental fluorine 15 min. All reactions at 2.0 mm, 40 cm^3 min^{-1} and 50 W for plasma treatment

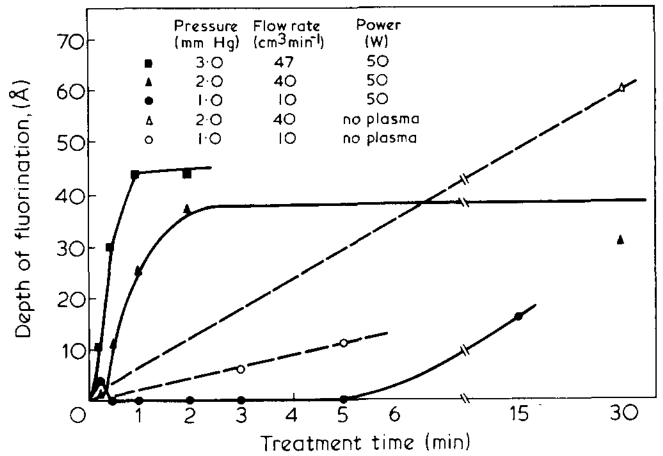

Figure 10 Depth of fluorination as a function of time of treatment for conditions of *Figure 2.* Notice the apparent higher depth of fluorination at higher pressures and flow rates

indication of the representative composition of the fluorinated layer. For the perfluorinated surfaces obtained in our experiments, we observe that Au_α is very close to 1341 while for those with small but measurable quantities of fluorine ($\sim 10\%$ F)Au_α is close to 1342.

Depth of fluorination. An important feature of the surface treated polyethylene samples is the depth of the perfluorinated layer obtained under various reaction conditions. An upper bound on this parameter can be obtained from the high resolution C_{1s} e.s.c.a. spectrum, typical examples of which were shown in *Figure 9*. From peaks (4) and (5) of *Figure 9*, we conclude that there is a small residual signal from CH_2–CH_2 moieties on the low binding energy side of the C_{1s} spectrum. This suggests that either all of the CH_2 groups within the first 50 Å (the depth probed by e.s.c.a.) have not been fluorinated or that the depth of perfluorination is less than 50 Å. We believe that the second explanation is more reasonable and conclude that the depth of fluorination is somewhat less than 50 Å in typical experiments.

Another estimate of the depth of fluorination can be obtained by the method suggested by Clark and coworkers[10] summarized in Appendix III. The depths of fluorination corresponding to the various treatment conditions described by the data of *Figures 2* and *6* are shown in *Figures 10* and *11* respectively. From these Figures it is apparent that the maximum depth of fluorination achievable under these conditions is $\sim$40 Å. *Figure 10* also suggests that at higher pressures and flow rates than employed here, the depth of fluorination may be greater. This is consistent with a mechanism of fluorination which is diffusion controlled. Increased pressure would correspond to a higher effective concentration of reactive species, thus increasing the concentration gradient for diffusion. Also from *Figures 10* and *11* we see that a flow rate of $\sim$40 cm^3 min^{-1} is necessary to obtain significant depths of fluorination at short reaction times.

The apparent upper limit on the depth of fluorination can be explained in terms of the etching behaviour of plasmas containing fluorine species. It has recently been found that unsaturated monomers such as C_2F_4, C_3F_6 etc. polymerize readily in the glow discharge but with saturated fluorocarbons such as CF_4, C_2F_6 little or no polymer formation occurs. The inability for the polymer to form is attributed to the competitive ablation and polymerization (*CAP*)[25,26] and ion-assisted etching[27,28] processes taking place. Polymerization can be achieved if the effective concentration of the fluorine ions, which cause etching, can be reduced. This is possible by addition of specific gases such as hydrogen so that a part of the fluorine ions are eliminated by the side reaction involving formation of HF. This, in effect, increases the C/F ratio of available reactive species in the system. In our study, the presence of fluorine alone would represent the extreme case of plasma etching because the C/F ratio would be zero, representing a completely ablative process. However, the presence of an inert gas such as helium (a 95% He, 5% F_2 premixture is being used), the ablation of some hydrocarbons from solid PE into the gas phase, and the reaction of fluorine with hydrogens eliminated from the polyethylene might all serve as effective diluents for reducing the etching capability of the fluorine plasma. In this respect, the reaction of PE with fluorine plasma would be significantly different from that of elemental fluorine. Also, etching in the case of plasma treatment would have the added advantage of removal of surface layers richer in oxygen, therefore providing the potential for reducing the oxygen levels on the surface to values lower than those for the original polyethylene substrate. If, as expected, the fluorine plasma is causing simultaneous chemical reaction and reactive ion etching from the surface, the depth of fluorination will be controlled by competition between the etching and chemical reaction in the plasma. It is apparent then, that under the reaction conditions studied, the depth of fluorination will be restricted to the observed value of $\sim$40–45 Å. The effect of flow rate can also explain the reduced equilibrium depth of fluorination at lower flow rates and pressures. Clark and Dilks[23] have suggested that decrease in flow rate will increase the partial pressure of ions and metastables in the plasma and hence tend to increase the etching capability of the plasma. At low flow rates, ($\sim$10 cm^3 min^{-1}), the etching rate would be expected to be much larger. This is depicted by a long initial time scale where there is little fluorination occurring on the surface (see *Figures 2* and *10*). Different etching rates at various flow rates would also lead to different equilibrium levels of depth of fluorination as shown in *Figure 10*.

We have independent observations to suggest that etching is taking place in the presence of the fluorine plasma in our system. Firstly, a small loss in weight (0.1–0.2%) of the fluorinated polymers was observed for all

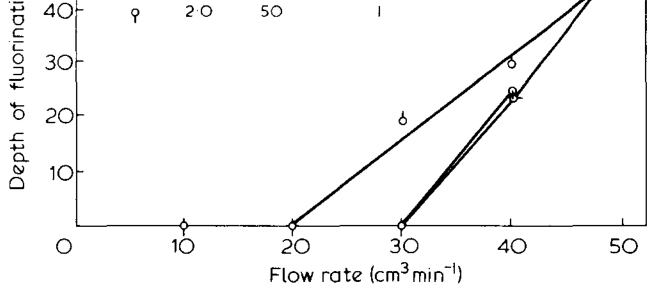

Figure 11 Depth of fluorination as a function of flow rate for reaction conditions corresponding to those in *Figure 6*

Table 4 Fluorination in the aluminium cage (Reaction conditions: Flow rate = 40 cm^3 min^{-1}; pressure = 3.0 mm; power = 50 W)

Time of treatment (min)	Atomic % from e.s.c.a. F	C	O	Approximate depth of fluorination (Å from e.s.c.a.)	Auger parameter
2	50.3	42.0	7.3	30	1341.2
5	54.9	40.3	4.8	38	1341.0
15	60.4	37.5	2.0	60	1340.9
60	58.9	37.1	4.1	59	1341.0
60*	58.6	37.3	4.1	35	1341.1

* No cage, only plasma

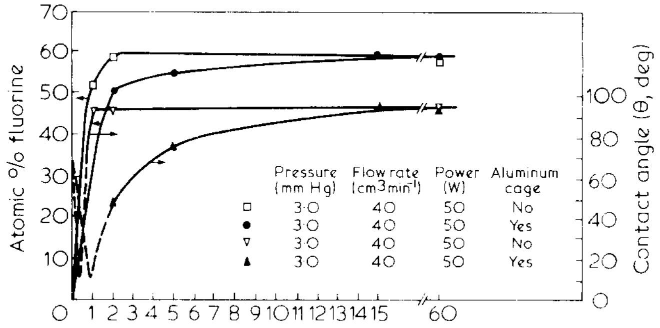

Figure 12 Comparison of fluorinations with and without the aluminum cage. Observe the reduction of reaction rate suggested by measurements of atomic percent fluorine and contact angle with formamide

reactions carried out at 1.0 mm and 10 cm^3 min^{-1}. However, at higher pressures and flow rates the sample weights remained almost constant. Secondly, a low molecular weight sticky material was found near the reactor exit; this material appeared to be partially fluorinated polyethylene as determined by infra-red measurements.

Fluorination of LDPE in an aluminium cage

The amount of etching could be reduced by elimination of ions from the reaction zone. This can be effectively achieved by either isolating the samples from the plasma by enclosing them in a Faraday cage (a grounded metal screen) inside the glow region or by carrying out the reactions in the dark region downstream of the plasma. In our study some reactions were carried out by isolating the samples in an aluminium screen. The screen was not grounded but it eliminated ions from near the reaction zone as evidenced by the glow around the screen but not inside. It is expected that the fluorine free radicals which have mean free paths smaller than the screen opening can diffuse through to the reaction zone.

In these experiments, the aluminium screen was slipped into the quartz reactor and around the sample carousel so that the specimens could be positioned at the same place with respect to the *rf* coil as in earlier reactions. The results of these fluorinations are summarized in *Table 4*. Comparison with reactions carried out in the absence of the cage are shown in *Figures 12* and *13*. There is a measurable increase in depth of fluorination to values greater than 60 Å, i.e. beyond the limit of analysis in our e.s.c.a. measurements (*Table 4*, *Figure 13*). The Auger parameter indicates that the surface composition obtained in the cage reactions is again similar to that of PTFE (*Table 4*), and essentially is identical to the surface composition obtained in the plasma treatments without the cage. However, the rate of reaction is reduced by about a factor of two, probably due to the elimination of reactive sites on the substrate when the cage is present. Contact angle measurements on samples treated within the metal screen again parallel the trend seen in e.s.c.a. measurements (*Figure 12*). Despite the increased depth of treatment by removal of fluorine ions, there seems to be a limit on the depth of fluorination even by this approach. It is likely that parameters controlling diffusion would impose such a limit.

One important observation not shown in the Figures or the Table is that in all aluminium cage experiments done under ion-depleted conditions an increase in weight was observed (~0.1 0.2%) which would be expected if there is little or no etching and if the hydrogen atoms are replaced by fluorine atoms. On this basis, the observed weight gains are consistent with fluorinated layers in the range 140 330 Å. It is important to re-emphasize that for experiments within the plasma at 1.0 mm, and in the absence of a cage, a loss in weight was observed.

Comparison of treated LDPE surfaces with the surface of polytetrafluorethylene. A crucial test in determining how closely the fluorinated layer resembles the surface of polytetrafluoroethylene (PTFE) lies in a direct comparison of their C_{1s} spectra as shown in *Figure 14*. It is important to point out that this is a plot of $N(E)$ vs. kinetic energy of the emitted C_{1s} photoelectrons. The binding energy can be obtained by subtracting the kinetic energy and shift in energy due to surface charging from the energy of the excitation source i.e. 1253.6 eV for Mg$K\alpha$ source. Since we are studying the effect of charging on chemical structure, the positions of peaks have not been moved to locations where they would actually occur in the absence or neutralization of charging effects. Several important features are seen. Firstly, for the plasma treated specimen, there is definitely some residual signal from partially fluorinated species in the range 960 965 eV. This can be attributed to signals from depths greater than that of the perfluorinated layer. Also, the C_{1s} spectra of fluorinated polyethylene specimens have line widths or full widths at half maximum (*FWHMs*) of 4.7 eV as compared to 3.2 eV for PTFE. The measured line widths for core levels may be described by[29]:

$$(\Delta E_m)^2 = (\Delta E_x)^2 + (\Delta E_s)^2 + (\Delta E_{cl})^2$$

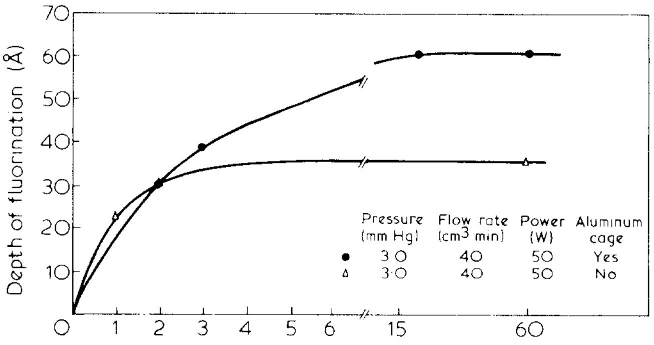

Figure 13 Build-up of fluorinated layer for reactions with and without the aluminum cage. A higher depth of fluorination for the cage conditions suggest reduced or no etching conditions

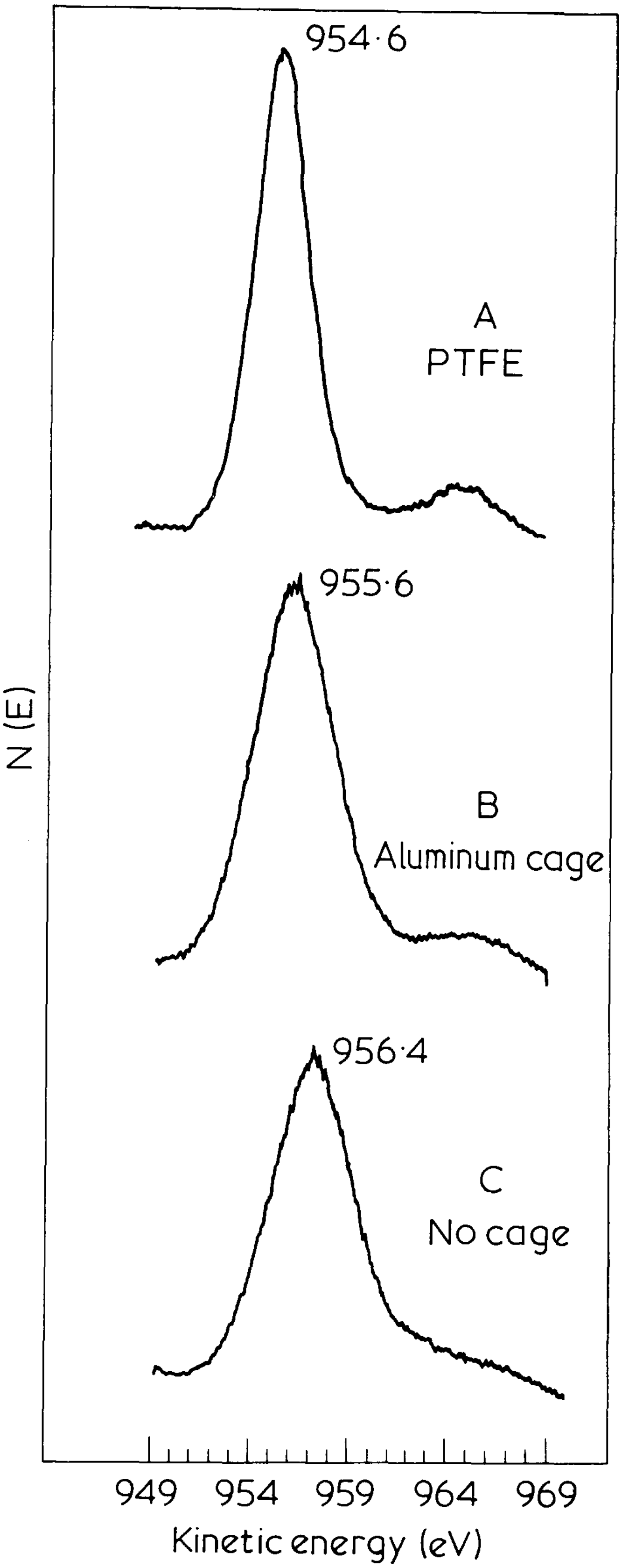

Figure 14 Comparison of C_{1s} spectra for reactions with and without the cage. Reaction conditions: 3.0 mm, 40 cm^3 min^{-1}, 60 min treatment, 50 W power. Observe peak widening, different equilibrium charging and line shape. The peaks at 965 eV are due to hydrocarbon build-up

where ΔE_m = measured width at half height, also called the full width at half maximum (*FWHM*); $\Delta E_x = FWHM$ of the photon source; ΔE_s = contribution to *FWHM* due to the spectrometer analyzer; and ΔE_{cl} = natural line width under investigation. For solids, ΔE_{cl} includes solid state effects related to differences in lattice environment thus leading to slightly differing binding energies. ΔE_x and ΔE_s would be constant in our case. The various lattice environment differences in the fluorinated polymers could arise from differences in chemical species, crystallinity and atom density. In terms of these three components, there are important differences between PTFE and fluorinated LDPE. Plasma fluorinated polymers contain ~4–5% oxygen-containing species and small amounts of $-CF_3$. Both these chemical components could increase the *FWHM*. The effect of differences in crystallinity between PTFE, LDPE and the fluorinated LDPE on *FWHM* are not known. The fluorinated polymer may be crosslinked near the surface, leading to a greater atom density on the surface. Again, the effect of this on *FWHM* is not known, though its effect on peak intensity has been studied[30]. If there are any partially fluorinated moieties in the surface layer, an increase in *FWHM* would be expected. Formation of such species could easily arise from different reactivities of crystalline and amorphous zones of the polyethylene.

In terms of equilibrium charging (in e.s.c.a. measurements) of these polymers, the equilibrium charge on PTFE is higher by 1 eV compared to the LDPE sample treated in the aluminium screen and is 1.8 eV higher than the sample treated in the absence of the cage (*Figure 14*). The various arguments involved in the discussion of FWHM would be applicable here too. Also, if several different species such as $-CF_3$, $-CF_2$, $-CHF$, $C=O$ are present, differential charging could result in an increase in *FWHM*.

The integrated areas of the C_{1s} peaks for the fluorinated polymers are higher than those for PTFE suggesting a crosslinked surface based on the observations first made by Clark and coworkers[30] for polyethylene treated with inert gas plasmas. Although not shown in *Figure 14*, the integrated areas for F_{1s} spectra were slightly lower for the treated polyethylene samples suggesting that the surface layer of the polymer is not completely fluorinated.

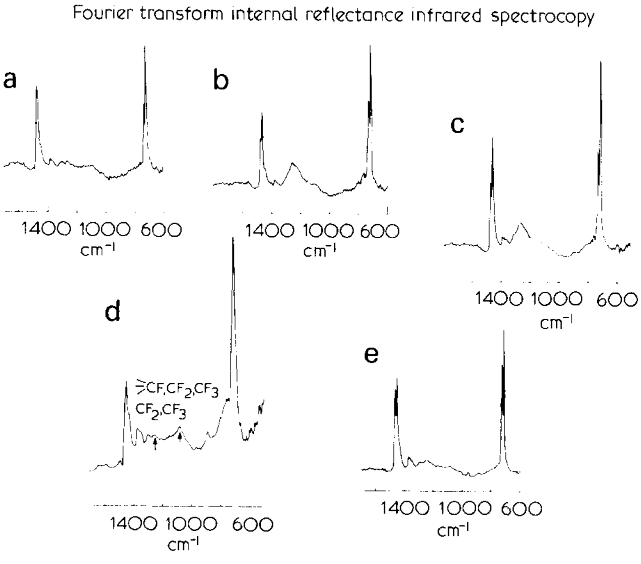

Figure 15 *FTMIR* spectra for reactions with and without aluminum screen (A.S) (a) 5 min, A.S (b) 15 min A.S (c) 60 min A.S (d) Plasma 5 min (e) Plasma 60 min; reactions at 3.0 min, 40 cm^3 min^{-1}, 50 W. Observe the little change in CF_2 peak height between 15 m and 60 min treatment in aluminum screen. Also notice the sharp drop in $-CF_2$ peak for 60 min plasma treatment, suggesting etching conditions

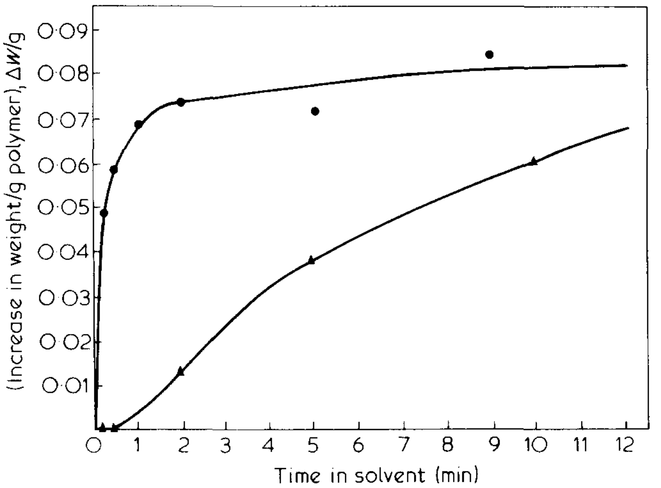

Figure 16 Solvent sorption in *p*-xylene at 25°C. Note initial period of no solvent uptake and the drop in slope for plasma treated polymer. ●, Untreated LDPE; ▲, plasma treatment: 2.0 mm, 40 cm^3 min^{-1}, 5 min

Surface infra-red spectroscopic measurements

Further characterization was carried out using *FTMIR* i.r. which, under the conditions employed, can give an average analysis to a depth of ~10000 Å. This technique is especially useful for identification of various chemical species and to obtain some indication of the depth of fluorination beyond the limit of e.s.c.a. Typical spectra are shown in *Figure 15*. These results show that the depth of fluorination is small although a quantitative estimate is not possible from our i.r. data. However, it is possible to observe the build-up of CF_2 species as the fluorination progresses (*Figures 15a, b, c* for metal cage; *d, e* without cage). There is no significant change in the size of the band associated with CF_2 type species for the cage experiments going from 15 to 60 min treatment. This supports the previous conclusion drawn from e.s.c.a. measurements concerning an upper limit on the depth of fluorination even with experiments under conditions of reduced ion concentration near the solid substrate. However, in the case of plasma treatment without the cage, comparison of 5 min treatment (*Figure 15d*) with 60 min treatment (*Figure 15e*) shows a decline in depth of fluorination. This is consistent with etching ideas. Small changes in reaction conditions could change the etching efficiency which in turn could lead to a reduction in depth of fluorination.

Another interesting feature of the *FTMIR* experiments lies in the comparison of the crystalline bands (731, 1473) and amorphous bands (720, 1463 cm^{-1}). Because of the change in the strength of these bands, changes in the surface crystallinity can be postulated[20,31,32]. It appears that the surface crystallinity of the plasma treated polyethylene (*Figures d* and *e*) is higher than for samples treated in the aluminium cage (*Figures a–c*). In the plasma treatment case, layers of less crystalline material are etched away from the surface, exposing the more crystalline region below. For example, the band at 731 is larger relative to that at 720 in *Figure 15e* compared to *Figure 15c*. However, if no etching takes place, as postulated for the case of reactions in the aluminium cage, the original degree of surface crystallinity is retained and possibly decreased during the reaction (*Figures 15a, b, c*).

Additional properties of the fluorinated polyethylene

The effectiveness of the polymer as a retardant to solvent diffusion was studied by monitoring the change in weight of the fluorinated film as a function of time in *p*-xylene at 25°C. The result of one particular experiment is shown in *Figure 16*. The curves of *Figure 16* indicate that the rate of solvent uptake was reduced by a factor of ~20 for the treated film.

Fluorination of polyethylene powders (~0.15 m^2 s^{-1} by BET measurement) was carried out in the fluidized bed reactor of *Figure 1b*. The major results of these experiments will be reported in future publications; some important observations are noted here. D.s.c. (20 K min^{-1} over the range 350–650 K) of the treated powders showed no change in the melting point of polyethylene, and did not reveal any significant features attributable to the fluorinated polymer. The treated powders could not be moulded under conditions which were suitable for the untreated polyethylene (150°C, 30 MPa). The treated powders could be preformed at 95°C and 60 MPa to allow for cold compacting at 350 MPa in an isostatic press. The properties of these compacted powders are being investigated at present.

The question of mechanical integrity and the ageing behaviour of the fluorinated polymers, especially treated in plasmas, is an important consideration. We find that contact angles and overall fluorine contents remain constant for perfluorinated surfaces over periods of several months. This is extremely important because plasma polymerized thin films of polytetrafluoroethylene and other plasma-polymerized films degrade with time due to post-reaction of trapped free radicals with atmospheric oxygen. This has been observed by several researchers[33,34], and is clearly a significant disadvantage compared to the surfaces prepared by the methods described here. The moulding characteristics of the plasma fluorinated powders reveal some information on the mechanical integrity of the fluorinated layer. The fact that powders did not compression mould at 150°C and 30 MPa suggests that the outer fluorinated and crosslinked layer does not rupture under these extreme conditions.

SUMMARY

Plasma treatment in the absence of a aluminium cage

(1) The first molecular layer is similar to PTFE if reaction goes to completion. There is also the likelihood of the presence of some terminal CF_3 groups in this layer.

(2) Depth of fluorination is of the order of 40 Å. The limitations on depth of fluorination appear to be related to simultaneous etching taking place in the plasma.

(3) CF_2 groups are rapidly generated in the plasma as determined by chemical shifts in the C_{1s} e.s.c.a. spectrum.

(4) For incomplete surface fluorination, there is a post-reaction with oxygen (O_2 or H_2O). No such reaction is observed for perfluorinated surfaces.

(5) The surface of the fluorinated polymer is crosslinked.

(6) The degree of surface crystallinity appears to be increased in the plasma treatment.

Treatment in the aluminium cage

(1) The first molecular layer is largely CF_2 interspersed with some CF_3 groups as determined by contact angle measurements.

(2) Depth of fluorination can be increased to ~60 Å by removal of fluorine ions which cause etching. It appears that diffusion limitations are responsible for the limit on the depth of fluorination.

(3) Chemical species in the surface and subsurface layers are largely $-CF_2$ type as determined by e.s.c.a. chemical shifts and Auger parameter.

(4) The polymer surface is crosslinked as in the case of plasma treatment.

(5) There is an apparent decrease in surface crystallinity with increase in reaction time.

Reaction kinetics

The rate of chemical reaction is dependent on the flow rate and the reaction pressure. An increase in either of these variables accelerates fluorination in the plasma. In the presence of the aluminium screen, however, the reaction rate decreases, possibly owing to absence of reactive sites on the solid substrate.

ACKNOWLEDGEMENT

This research is supported by the National Science Foundation, Division of Engineering.

REFERENCES

1 Rudge, A. J. Br. Pat. 710 523 (1952)

2 Schonhorn, H., Gallagher, P. K., Luongo, J. P. and Padden, F. J. Jr., *Macromolecules* 1970, **3**, 800

3 Tanner, K. *Chimia* 1968, **22**, 197

4 Brown, D. W., Florin, R. E. and Wall, L. A. *Appl. Polym. Symp.* 1973, **22**, 169

5 Lagow, R. J. and Margrave, J. L. *J. Polym. Sci. Polym. Lett. Edn*, 1974, **12**, 177

6 Hayes, L. J. and Dixon, D. D. *J. Appl. Polym. Sci.* 1979, **23**, 1907

7 Gerhardt, G. E., Dumitru, E. T. and Lagow, R. J. *J. Polym. Sci., Polym. Chem. Edn* 1979, **18**, 157

8 Fredericks, P. S. and Tedder, J. M. *J. Chem. Soc.* 1960, 144

9 Shimada, Junichi and Hoshino, Mitsutoshi, *J. Appl. Polym. Sci.* 1975, **19**, 1439

10 Clark, D. T., Feast, W. J., Musgrave, W. K. R. and Ritchie, I. *J. Polym. Sci. Polym. Chem. Edn* 1975, **13**, 857

11 ibid, *ACS Org. Coat. Plast. Chem. Prepr.* 1974, **34**(1), 307

12 Yasuda, H. and Hsu, T. S. *J. Polym. Sci., Polym. Chem. Edn* 1978, **16**, 415

13 Nakajima, K., Bell, A. T. and Shen, M. *J. Appl. Polym. Sci.* 1979, **23**, 2627

14 Rice, D. W. and O'Kane, D. F. *J. Electrochem. Soc., Electrochem. Sci. Tech.* 1976, **123**(9), 1308

15 Kay, E., Dilks, A. and Hetzler, U. *J. Macromol. Sci.-Chem.* 1978, **A12**(9), 1393

16 Manion, J. P. and Davies, D. J. US Pat. 3 674 667 (1972)

17 Wagner, C. D., Riggs, W. M., Davis, L. E., Moulder, J. F. and Muilenberg, J. E. 'Handbook of XPS', Perkin Elmer, Physical Electronics, 1979

18 Clark, D. T. and Shuttleworth, D. *J. Polym. Sci., Poly. Chem. Edn* 1980, **18**, 27

19 Harrick, N. J. *J. Phys. Chem.* 1960, **64**, 1110

20 Luongo, J. P. and Schonhorn, H. *J. Polym. Sci. Part A-2* 1968, **6**, 1649

21 Blackadder, D. A. and Vincent, P. I. *Polymer* 1974, **15**(1), 2

22 Berens, A. R. *Polymer* 1977, **18**, 699

23 Clark, D. T and Dilks, A. *J. Polym. Sci., Polym. Chem. Edn* 1978, **16**, 911

24 Kaelble, D. H. 'Physical Chemistry of Adhesion', Wiley, New York, 1971

25 Masuoka, T., Yasuda, H. and Morosoff, N. *ACS Polym. Prepr.* 1978, Sept, 498

26 Yasuda, H. *ACS Polym. Prepr.* 1978, **Sept**, 491

27 Matsuo, Seitaro and Takehara, Yumiko, *Japan J. Appl. Phys.* 1977, **16**, 175

28 Coburn, J. W., Winters, H. F. and Chuang, J. *J. Appl. Phys.* 1977, **48**, 3532

29 Clark, D. T. in 'Electron Emission Spectroscopy' (Ed. W. Dekeyser *et al.*) D. Reidel, Dordrecht-Holland, 1973

30 Clark, D. T. and Dilks, A. *J. Polym. Sci., Polym. Chem. Edn* 1977, **15**, 2321

31 Luongo, J. P. *J. Polym. Sci., Polym. Chem. Edn* 1974, **12**, 1203

32 Hart, W. W. and Koenig, J. *Adv. Chem. Ser.* 1979, **174**

33 Kronick, P. L., Jesch, K. F. and Bloor, J. E. *J. Polym. Sci.* 1969, **A-1**, 767

34 Neiswender, D. D. *Adv. Chem. Ser.* 1969, **80**, 338

APPENDIX I

Atomic analysis using sensitivity factors[17]

For homogeneous samples in the analysis volume, the number of photoelectrons per second in a specific spectral peak is:

$$I = NF\alpha\theta y\lambda AT$$

where N = number of atoms in volume element; F = X-ray flux; α = cross-section for photoionization; θ = angular efficiency factor; y = efficiency in photoelectron formation process; λ = mean free path; A = area of sample from which photoelectrons are detected; and T = detection efficiency of electrons. Therefore

$$N = I/F\alpha\theta y\lambda AT = I/S$$

where S = atomic sensitivity factor. For two elements

$$\frac{N_1}{N_2} = \frac{I_1/S_1}{I_2/S_2}$$

Thus, atom fraction of any constituent in a sample is:

$$C_x = \frac{N_x}{\sum_i N_i} = \frac{I_x/S_x}{\Sigma I_i/S_i}$$

The atomic sensitivity values employed in our calculations are:

$$S_{\text{carbon}} = 0.205, \qquad S_{\text{oxygen}} = 0.63, \qquad S_{\text{Fluorine}} = 1.0$$

as obtained from Wagner *et al.*[17].

APPENDIX II

Table: Binding energies corresponding to various chemical species

Structure	Binding energy	Reference
$(\overset{*}{C}H_2-CH_2)$ bulk	285.0	(10)
$\overset{*}{C}H_2-CHF$	285.9	(10)
$\overset{*}{C}H_2-CF_2$	286.4, 286.6	(10,13)
$CHF-\overset{*}{C}H_2-CHF$	286.4	(10)
$>\overset{*}{C}=O$	287.9	(10)
$\overset{*}{C}HF-CH_2$	287.9, 288.0	(10,13)
$\overset{*}{C}HF-CHF$	289.0, 288.4	(10,13)
$\overset{*}{C}HF-CF_2$	289.3	(13)
$CH_2-\overset{*}{C}F_2$	290.7	(10)
$CHF-\overset{*}{C}F_2$	291.6	(13)
$\overset{*}{C}F_2-CF_2$	291.6, 292.2	(10,13)
$CHF(\overset{*}{C}F_3)CF_2$	293.7	(13)
$\overset{*}{C}F_3CF_3$	294.0	(13)

APPENDIX III

Calculation of fluorination thickness

As derived by Clark *et al.*[10] intensity of electrons of a given energy emitted in a homogeneous material by activation with an X-ray photon source

$$\mathrm{d}I = F\alpha N K e^{-x/\lambda}\mathrm{d}x$$

where $\mathrm{d}I$ = intensity arising from the layer of the surface between depths x and $x+\mathrm{d}x$; F = X-ray flux; α = cross-section for photoionization in a given shell of a given atom for a given X-ray energy; N = number of atoms in volume element; K = spectrometer factor; and λ = mean free path of electron. Integration with appropriate limits yields

$$I_d = I_\infty(1 - e^{-d/\lambda})$$

I_∞ = intensity from an infinitely thick layer; I_d = intensity from surface layer of thickness d.

Therefore, intensities of F_{1s} and F_{2s} peaks may be written as:

$$I_{F_{1s}} = I_{\infty F_{1s}}(1 - e^{-d/\lambda_1})$$

$$I_{F_{2s}} = I_{\infty F_{2s}}(1 - e^{-d/\lambda_2})$$

Thus,

$$\frac{I_{F_{1s}}}{I_{F_{2s}}} = \frac{I_{\infty F_{1s}}(1 - e^{-d/\lambda_1})}{I_{\infty F_{2s}}(1 - e^{-d/\lambda_2})}$$

$I_{F_{1s}}$, $I_{F_{2s}}$ are proportional to areas measured for F_{1s} and F_{2s} signals for a specimen. $I_{\infty F_{1s}}$, $I_{\infty F_{2s}}$ are proportional to areas measured for F_{1s} and F_{2s} signals for an infinite sample such as PTFE. Approximate values of λ_1, λ_2 are available in literature[10].

This expression can be rewritten as:

$$\frac{y}{k} - 1 = \frac{y}{k} e^{-d/\lambda_2} - e^{-d/\lambda_1}$$

where y = intensity ratio of F_{1s} and F_{2s} for sample and k = intensity ratio of F_{1s} and F_{2s} for the standard, PTFE.

Values of k, λ_1, λ_2 employed in our calculations are 11.25 Å, 8 Å and 14 Å respectively.